ELSEVIER

Journal of Chromatography A, 952 (2002) 85–98

JOURNAL OF CHROMATOGRAPHY A

www.elsevier.com/locate/chroma

Effect of salt gradients on the separation of dilute mixtures of proteins by ion-exchange in simulated moving beds

Joukje Houwing, Stef H. van Hateren, Hugo A.H. Billiet, Luuk A.M. van der Wielen*

Kluyver Laboratory for Biotechnology, Delft University of Technology, Julianalaan 67, 2628 BC Delft, The Netherlands

Received 19 July 2001; received in revised form 16 January 2002; accepted 24 January 2002

Abstract

Salt gradients can improve the efficiency during fractionation of proteins by ion-exchange in simulated moving beds (SMBs). The gradients are formed using feed and desorbent solutions of different salt concentrations. The thus introduced regions of high and low affinity may reduce eluent consumption and resin inventory compared to isocratic SMB systems. This paper describes a procedure for the selection of the flow-rate ratios that enables successful fractionation of a dilute binary mixture of proteins in a salt gradient. The procedure is based on the so-called ''triangle theory'' and can be used both for upward gradients (where salt is predominantly transported by the liquid) and downward gradients (where salt is predominantly transported by the sorbent). The procedure is verified by experiments. © 2002 Published by Elsevier Science B.V.

Keywords: Salt gradient; Simulated moving beds; Flow selection; Proteins

1. Introduction

Simulated moving bed (SMB) technology, a countercurrent chromatographic separation technique, is increasingly popular for chromatographic fractionation of various biotechnological and pharmaceutical mixtures. Many studies concern the fractionation of enantiomers for use as chiral drugs [1,2]. Other examples are the separation of amino acids [3] and antibiotics [4]. Advantages of the SMB over fixed-bed chromatography are an increased efficiency during separation of like molecules, reduction of the consumption of sorbent and reduction of the consumption of buffers [5].

In order to achieve the desired degree of separation in SMB, correct selection of the liquid and solid-phase flow-rates is crucial. The selection of the liquid to sorbent flow-rate ratios has been studied extensively. In most studies, the analogy between true moving bed (TMB) and SMB is exploited. Wave theory is then used to select the flow-rate ratios [6,7]. The most current method for flow-rate ratio selection is ''triangle theory'', as developed by the group of Morbidelli [7].

A novel development in SMB technology is the use of gradients in solvent strength. The gradient is formed by the use of a desorbent and feed solution of different modulator concentration. It introduces regions of high and low affinity of the solutes towards the resin in the SMB. When the top sections (sections III and IV in Fig. 1) have a high affinity, a high feed flow-rate can be applied. This is highly beneficial to

*Corresponding author. Fax: +31-15-278-2355.

E-mail address: l.a.m.vanderwielen@tnw.tudelft.nl (L.A.M. van der Wielen).

0021-9673/02/$ – see front matter
PII: S0021-9673(02)00091-2

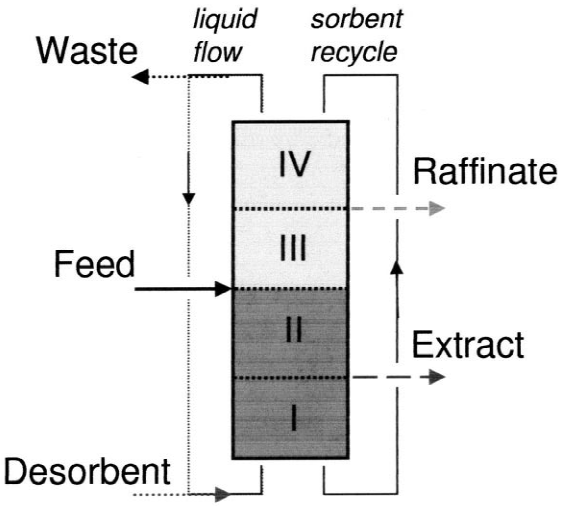

Fig. 1. Schematic representation of gradient in SMB and numbering of sections therein. A dark color indicates a low affinity of the protein for the matrix.

the throughput, the volume of feed that can be processed per resin volume. When the bottom sections (sections I and II in Fig. 1) have a low affinity, a low desorbent flow-rate suffices to regenerate the sorbent. Thus, the gradient increases throughput and reduces solvent consumption in comparison to the isocratic situation.

Examples of gradients in SMB systems are in the separation of sugars using temperature gradients [8], in supercritical fluid chromatography using pressure gradients [9], in reversed-phase separation of antibiotics, using methanol gradients [4], and in ion-exchange separation of proteins, using salt gradients [10].

In this paper we will further elaborate the protein separations in SMB aided by salt gradients. In general, the affinity of proteins towards the resin is reduced by increasing the salt concentration [11–13]. In a previous paper [14], the positioning of the salt gradient in the SMB has been addressed for salts interacting with the sorbent. The gradient can have two forms, namely an ''upward gradient'', where salt is predominantly transported by the liquid towards the top of the system (section IV) and as an ''downward gradient'', where salt is predominantly transported by the sorbent towards the bottom (section I).

In the current paper, we have applied the salt gradient SMB for separation of dilute mixtures of two proteins, namely bovine serum albumin (BSA) and myoglobin (myo). The procedure for selection of the flow-rates is extended to the presence of proteins. The predictions are verified by experiments.

2. Theory

The current methods for selection of the relative flow-rates in an SMB assume local equilibrium. They rely on the quantitative understanding of the equilibrium distribution coefficient of solutes over the liquid and sorbent phase. When separating dilute binary mixtures of proteins in a gradient SMB, the current method of selection of flow-rate ratios needs to be adjusted at some points:

1. Solutes substantially differ in size, which leads to a combination of size exclusion and ion-exchange mechanisms;
2. The strong relation between the flow-rate ratio, salt concentrations, and protein and salt distribution coefficients in all sections demands an integral approach for flow-rate selection.

In the following, we have assumed that the ion-exchange of proteins does not influence the distribution of salt on the ion-exchange resin, because diluted solutions of proteins were used.

2.1. Size exclusion and ion exchange

The three solutes considered, two proteins and a salt, are different in their molecular mass. Due to size-exclusion effects, the volume fraction of the sorbent particle that is accessible to the large protein molecules is much smaller than the fraction accessible to the small salt molecule. We treated this situation by assuming that:

- Liquid flow only occurs in the void fraction (ϵ_b) of the particle bed;
- The pore liquid always contains the same salt concentration as the bulk liquid, as a result of very fast diffusion;
- The average concentration in the particle q^* is determined by the pores, filled with the liquid concentration c and the resin of the concentration q, which is in ion-exchange equilibrium with the pore liquid:

$$q^* = \epsilon_p c + (1 - \epsilon_p) q \quad (1)$$

Several models have been developed to describe the ion-exchange equilibrium of the proteins and the ion-exchange matrix. Examples thereof are the mass action model of Kopaciewitz et al. [11], a similar model that includes size exclusion [12], the steric mass action (SMA) model [13], which includes the steric blocking of ion-exchange sites by the bulky protein molecule, and the extension to the SMA model that incorporates the pH-dependence of the ion-exchange equilibrium [15]. At the low protein concentrations used in this study, the models lead to very similar results. Hence, we used the simplest mass action description of the ion-exchange equilibrium [11]. Ion exchange is then regarded as an reaction of a characteristic number of charges, z_p, of a protein (P) with as many salt ions bound to the ion-exchanger (RX), where the protein is bound ($R_{z_p}P$) and the salt ions (X^-) are released into solution:

$$P^{z_p-} + z_p RX^- \Leftrightarrow R_{z_p}P + z_p X^-$$

Hence, the equilibrium distribution coefficient of protein over sorbent and liquid depends on the concentration of salt. In case of dilute solutions, where competition between proteins for exchange sites is absent, the distribution coefficient K_{IEX} ($= q_p/c_p$) can be written as:

$$K_{IEX} = K_0 c_s^{-z_p} \quad (2)$$

where K_0 is a reference distribution coefficient in a 1 *M* salt solution and c_s is the concentration of salt.

The values of K_0 and z_p are determined experimentally from the residence times of pulses of protein at varying salt concentrations. The exact procedure is described by Kopaciewitz et al. [11].

The overall equilibrium constant is defined as:

$$K_i = \epsilon_p + (1 - \epsilon_p) \cdot K_{0,i} c_s^{-z_i} \quad (3)$$

where i denotes either of the two proteins.

The distribution of salt over the ion-exchange resin and the liquid is assumed to be governed by a mechanism based on Donnan interaction, as has been described elsewhere [14]. At low concentration, co-ions are excluded from the resin as a result of Donnan repulsion, but at high concentration, charges are shielded and the entire salt ''molecule'' can enter the resin. In case of a salt consisting of two single-valent ions, such as sodium chloride, the resulting isotherm equation is:

$$\frac{q_s}{Q} = -0.5 + 0.5\sqrt{1 + 4S\left(\frac{c_s}{Q}\right)^2} \quad (4)$$

A similar equation can be derived for multivalent ions, such as calcium chloride or sodium sulfate, as well as for reactive buffer systems, such as acetic acid buffers [16].

The previously reported parameters for sodium chloride in a 10 m*M* Tris buffer at pH 8.0 on a Q-Sepharose FF ion-exchange matrix are $S = 1.09$, $Q = 0.22$. Tris and salt have been regarded as one species, since the salt concentration (200–500 m*M*) largely exceeded the Tris concentration (10 m*M*).

2.2. Region of complete separation

In order to select the liquid to sorbent flow-rate ratios that lead to complete separation of the feed, an extended version of the ''triangle theory'' as developed by Morbidelli et al. [7] has been developed. Key parameters are the liquid to sorbent flow-rate ratios *m*, which can be calculated from the SMB flow-rates Φ^{SMB}, switch time τ, column volume *V* and dead volume per column V_d by [17]:

$$m = \frac{\Phi^{SMB}\tau - V\epsilon - V_d}{V(1 - \epsilon)} \quad (5)$$

The flow-rate ratios are constrained by $m_j = K(c_{s,j})$, where m_j is the flow-rate ratio in section *j* and $K(c_{s,j})$ is the ''distribution coefficient'' of salt or protein as a function of the salt concentration c_s in section *j* [10,14]. The constraints thus are implicit relations of the salt concentrations in all sections. In dilute systems, where ion-exchange of proteins does not influence the salt distribution, the salt concentrations can be calculated from the mass balances over the points of feed and desorbent entry. In the following, we assume there is no recycle of the liquid leaving section IV to the desorbent, a so-called ''open loop system''. Also, we impose that the gradient is properly established, hence the concentrations in the lower sections I and II are equal and denoted as c_{II}, and the concentrations in the upper

sections III and IV are also equal and denoted as c_{III}. Imposing the correct gradient is similar to imposing complete separation to calculate the region of complete separation. A mass balance over the part of the SMB between the middle of section II and the middle of section III then reads:

$$m_2 c_{II} + (m_3 - m_2)c_F - m_3 c_{III} + q_{III} - q_{II} = 0 \qquad (6)$$

We will further refer to this equation as the feed balance. The first three terms represent the salt entering via the liquid in section II, entering via the feed at concentration c_F, and leaving via the liquid from section III. The last two terms represent salt entering via the sorbent in section III and leaving via the sorbent in section II. In all sections, equilibrium between the liquid and sorbed phases is assumed.

At this point, the choice between an upward or downward gradient needs to be made. In case of an upward gradient, the salt concentration in the lower sections c_{II} equals the desorbent concentration c_D. The concentration in the upper sections c_{III} is computed from Eq. (6).

In case of a downward gradient, none of the concentrations c_{II} and c_{III} is known. To find all salt concentrations, an additional mass balance is required. This balance is over the top of the SMB, over the part limited by the middle of section IV and the middle of section I [14]:

$$m_1(c_D - c_{II}) + q_{II} - q_{III} = 0 \qquad (7)$$

where the first term represents the salt entering section I via the liquid as desorbent and leaving via the liquid; the latter terms represent the salt entering via the sorbent from section II and leaving to section IV. The consequence of Eq. (7) is, that m_1 needs to be specified before the constraints to the operating region can be found.

With the obtained salt concentrations, the boundaries of the operating region are identified. As correct movement of all components needs to be assured, three boundaries $m_j = K(c_{s,j})$ are found per section; one for each component. Sometimes, a limiting boundary has to be identified from two minimum or maximum boundaries. This is dealt with in the following manner:

- The limiting maximum flow-rate ratio equals the smallest distribution coefficient at the local salt concentration of the components moving downward. Once this component of smallest retention moves downward, all other components with higher retention will surely move downward.
- The limiting minimum flow-rate ratio equals the largest distribution coefficient at the local salt concentration. Whenever the most retained component moves upward, all components of lower retention will surely move upward.

Salt has a convex curved isotherm, so salt fronts can either be diffuse (during loading of a column with a solution of increased salt concentration) or a shock (during elution with a solution of decreased salt concentration) [18]. It is important to take the correct front shape into account, since shock and diffuse waves move at different velocities. Further details on salt positioning are described elsewhere [14].

The completed results of the procedure for flow-rate ratio selection are shown in Table 1. There, $(\partial q/\partial c)_c$ denotes a diffuse front at the concentration c, $(\Delta q/\Delta c)_{c_1-c_2}$ denotes a shock front between concentrations c_1 and c_2, and c_j is the salt concentration in section j. By simultaneous solution of the mass balance Eqs. (6) and (7) and the equations of limiting flow-rate ratios in Table 1, the constraints to the flow-rate ratios are found.

Using the criteria on m_2 and m_3, a region of complete separation in the $m_2 - m_3$ plane is constructed, analogous to ''triangle theory''. When operating points are chosen within the defined region, separation of the two protein components in sections II and III is guaranteed.

2.3. Regeneration of desorbent and sorbent

Optimal operation of the SMB in terms of desorbent use, and purity and recovery of the extract and raffinate products requires regeneration of the sorbent in section I and of the desorbent in section IV. The purpose is to remove the proteins, while not disturbing the salt gradient. This is established by careful selection of the flow-rate ratios m_1 and m_4. That is not a trivial task, since conflicting situations may occur in section IV in an upward gradient and in section I in a downward gradient.

The regeneration of the desorbent in section IV in an upward gradient requires that salt moves upward

Table 1
Flow-rate ratio constraints in upward and downward gradients. (A) less retained protein, (B) more retained protein. The salt concentration in section II, c_{II} and section III, c_{III}, are calculated from the mass balance Eqs. (1) and (2)

	Upward gradient		Downward gradient	
	Lower boundary	Upper boundary	Lower boundary	Upper boundary
m_1	Maximum of $\left(\frac{\partial q}{\partial c}\right)_{c_D}$, $K_A(c_D)$	–	$K_A(c_{II})$	$\left(\frac{\Delta q}{\Delta c}\right)_{c_D-c_{II}}$
m_2	Maximum of $\left(\frac{\partial q}{\partial c}\right)_{c_D}$, $K_A(c_D)$	$K_B(c_D)$	$K_A(c_{II})$	$\left(\frac{\Delta q}{\Delta c}\right)_{c_D-c_{II}}$, $K_B(c_{II})$
m_3	Minimum of $\left(\frac{\Delta q}{\Delta c}\right)_{c_D-c_{III}}$, $K_A(c_{III})$	$K_B(c_{III})$	$K_A(c_{III})$	Minimum of $\left(\frac{\partial q}{\partial c}\right)_{c_{III}}$, $K_B(c_{III})$
m_4	Maximum of $\left(\frac{\Delta q}{\Delta c}\right)_{c_D-c_{III}}$	$K_A(c_{III})$	–	Minimum of $\left(\frac{\partial q}{\partial c}\right)_{c_{III}}$, $K_A(c_{III})$

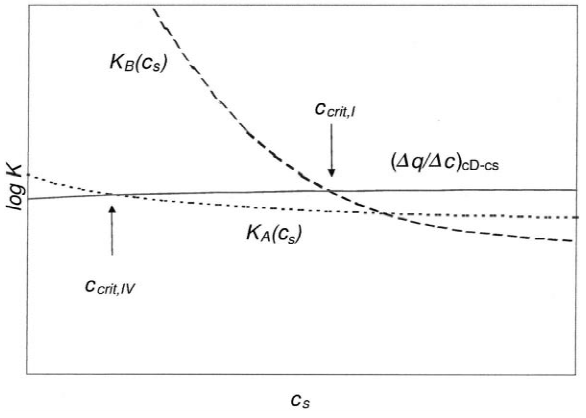

Fig. 2. Typical example of distribution coefficients of proteins as a function of salt concentration and definition of critical concentrations.

and the two proteins move downward in section IV. A conflicting situation occurs when the plots of the distribution coefficients of salt and protein as a function of the salt concentration intersect. A typical example of this azeotropic situation [10] is shown in Fig. 2. Components A and B are two arbitrary proteins, of which the distribution coefficients $K_A(c_s)$ and $K_B(c_s)$ have been plotted as a function of the salt concentration. According to Table 2, the salt distribution coefficient in section IV is represented by $(\Delta q/\Delta c)_{c_D-c_{III}}$. In the figure, c_D is constant and c_{III} is variable. The lines of the distribution coefficient of the less retained protein A and salt intersect at $c_{crit,IV}$. Only at concentrations below $c_{crit,IV}$, it is possible to find a flow-rate ratio that results in downward movement of the less retained protein [i.e.

Table 2
Distribution coefficients of BSA and myoglobin on Q Sepharose FF, in 10 m*M* Tris buffer, pH 8

Component	Isotherm	Parameters			
Protein	$K = \epsilon_p + (1-\epsilon_p)K_0 c_s^{-z_p}$	Component	ϵ_p	K_0	z_p
		BSA	0.49	$1.61\cdot10^{-3}$	5.61
		myoglobin	0.64	$0.76\cdot10^{-3}$	1.31
Salt	$\frac{q_s}{Q} = -\frac{1}{2} + \frac{1}{2}\sqrt{1+4S\left(\frac{c_s}{Q}\right)^2}$	Component	Q	S	
		NaCl	0.22	1.09	

$m < K_A(c_s)$] and simultaneous upward movement of the salt [i.e. $m > (\Delta q/\Delta c)_{c_D - c_{III}}$].

Obviously, regeneration of the desorbent will only occur when c_{III} exceeds $c_{crit,IV}$. This implies the feed concentration has to be below that critical concentration. As the flow-rate ratios, m_2 and m_3 also determine the concentration c_{III}, these are also restricted. An additional boundary to the region of complete separation is found by imposing the critical concentration in section IV. This concentration is found by equating the distribution coefficient of salt and protein A, at the chosen desorbent concentration. The supporting flow-rate ratios are calculated from the feed mass balance (6). Thus, a straight line is obtained:

$$m_3 = \frac{m_2(c_D - c_F) + q_{crit,IV} - q_D}{c_{crit,IV} - c_F} \quad (8)$$

In order to regenerate the sorbent in section I in a downward gradient, upward movement of all proteins and downward movement of salt is required in that section. A conflicting situation occurs when the lines of the salt and protein distribution coefficients intersect as a function of the salt concentration. According to Table 2, the distribution coefficient of salt is then given by $(\Delta q/\Delta c)_{c_D - c_{II}}$. In Fig. 2, the salt distribution coefficient is plotted at constant c_D and variable c_{II}. At $c_{crit,I}$, the distribution coefficients of the more retained protein A and salt are equal. Only if the salt concentration c_{II} exceeds this critical salt concentration of section I, $c_{crit,I}$, salt can move downward [by choosing $m < (\Delta q/\Delta c)_{c_D - c_{II}}$] and proteins move upward [by choosing $m > K_B(c_s)$]. Else, both B and salt move downward.

The requirement to achieve the critical concentration in section I imposes that the feed concentration has to exceed $c_{crit,I}$ and that the flow-rate ratios m_2 and m_3 support that concentration. An additional boundary to the region of complete separation is found by imposing the critical concentration in section I, and then calculating the supporting flow-rate ratios from the mass balances (6) and (7). By imposing a constant c_{II}, c_{III} is also fixed. Thus, a straight line of m_3 as a function of m_2 is obtained:

$$m_3 = \frac{m_2(c_{crit,I} - c_F) + q_{III} - q_{crit,I}}{c_F - c_{III}} \quad (9)$$

3. Experimental

3.1. Materials

In this study, a synthetic mixture of myoglobin from horse heart (Sigma, Cat. no. M1882, >90% pure, Sigma–Aldrich, Zwijndrecht, The Netherlands) and bovine serum albumin (Sigma, Cat. no. A7906, Sigma–Aldrich) was used as a feed solution. All solutions were based on a 10 m*M* Tris buffer, pH 8.0, to which sodium chloride was added for controlling the salt concentration. All salts were obtained from Merck (Darmstadt, Germany). The sorbent, Q-Sepharose FF, was obtained from Amersham Pharmacia Biotech (Uppsala, Sweden). This strong ion-exchange matrix, based on highly cross-linked agarose has an average particle size of 90 μm and a capacity for small ions of 200 m*M* [19].

3.2. Columns

Columns were packed according to the procedure described by the manufacturer [19]. One Pharmacia XK16 column of 14.5 ml volume was used for isotherm determination on a Pharmacia FPLC system. In the laboratory-scale simulated moving bed, the sorbent was packed in 1-cm diameter Omnifit glass columns to a column volume of 7.1 ml. The packing quality of these columns was checked by determination of the breakthrough of a salt solution.

3.3. SMB system

The SMB system used for experiments has been described elsewhere [20]. The concentrations of the two proteins in the system were calculated from the adsorbance at 280 and 405 nm, as determined by an in-line Shimadzu SPD-M10Avp photo-diode array detection system, operated under CLASS-VP software (version 4.2, Shimadzu). The dead volume of the assembled system was determined by breakthrough experiments of salt on the system without columns attached at 0.38 ml per column.

3.4. Determination of isotherm

The proteins' characteristic charges and reference equilibrium constants were determined from reten-

tion times of pulses at varying concentrations of salt, analogous to the method described by Kopaciewitz et al. [11]. The injected pulses of 100 μl contained solutions of 10 g/l BSA or 1.0 g/l myoglobin, with a salt concentration adjusted to the eluent concentration. Experiments were carried out at a flow-rate of 2 ml/min.

The data obtained by pulse experiments were verified by breakthrough experiments. A solution of either 0.5 g/l BSA or 0.1 g/l myoglobin was applied at 3 ml/min onto the column equilibrated during 5 column volumes. The equilibration buffer and the sample contained the same salt concentration in the range of 200–300 m*M* NaCl. After loading, the column was regenerated using a 1 *M* NaCl solution.

The isotherm of sodium chloride on Q-Sepharose FF has been described elsewhere [14].

3.5. SMB experiments

During operation of the system, the recycle stream was wasted, instead of being reused for further reduction of consumption of eluent.

Before the experiment, columns were regenerated using 1 *M* NaCl and preferably re-equilibrated with 0.22 *M* NaCl. The best results were obtained by first running the SMB using a feed solution only containing salt. After about four cycles, when the salt gradient was formed, the feed was switched to the protein containing solution. By this procedure, long lasting start-up effects were avoided.

3.6. Numerical procedures

Breakthrough profiles were simulated by numerical integration of the mass balance equations of liquid and sorbent phase, wherein mass transfer is approximated using a linear driving force approximation:

$$\frac{\partial c}{\partial t} = -v\frac{\partial c}{\partial x} + E\frac{\partial^2 c}{\partial x^2} - \beta k_o a(q_{eq} - q)$$
$$\frac{\partial q}{\partial t} = k_o a(q_{eq} - q) \qquad (10)$$

where q_{eq} is the solid-phase concentration in equilibrium with liquid concentration c, v is the interstitial velocity, β is the phase ratio $[(1-\epsilon)/\epsilon]$ and a is the specific interfacial area $(=6/d_p$, where d_p is the particle diameter). The mass transfer coefficient k_o was calculated from dimensionless relations, as described previously [20]. The used diffusion coefficients in free liquid were $D_{BSA} = 6\cdot10^{-11}$ m^2/s and $D_{myo} = 10.8\cdot10^{-11}$ m^2/s. The solids diffusion coefficients were $D_{p,BSA} = 0.73\cdot D_{BSA}$ and $D_{p,myo} = 0.84\cdot D_{myo}$, as cited in that paper.

The model, programmed in MATLAB, uses spatial discretization and a fourth order Runge Kutta algorithm for numerical integration. Axial dispersion was approximated by numerical dispersion.

The operating region was constructed by repeatedly simultaneous solving of the mass balance Eqs. (1) and (2) and the flow-rate criteria (Table 1), at chosen values of m_1 (only at downward gradient), and m_2 or m_3, using the optimization toolbox of MATLAB.

Steady state TMB profiles were calculated using an equilibrium stage model as described before [14,8]. Profiles were obtained by simultaneously solving the mass balances of all equilibrium stages, using the optimization toolbox of MATLAB.

4. Results and discussion

4.1. Distribution coefficients

Pulse experiments revealed that the ion-exchange equilibrium coefficient of BSA on Q-Sepharose FF at pH 8.0 strongly depends on the salt concentration (see Fig. 3). The slope of the line, i.e. the charac-

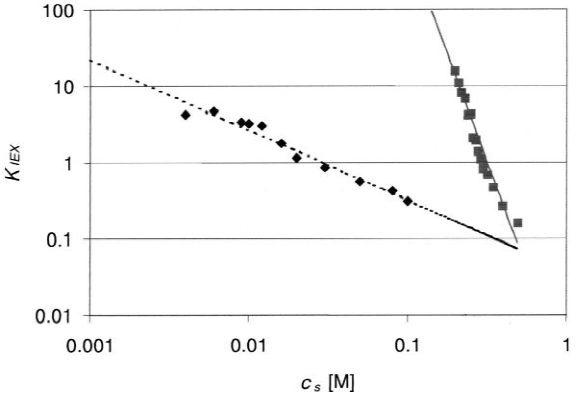

Fig. 3. Measured (points) and correlated (lines) ion-exchange isotherms of BSA (■) and myoglobin (♦) in 10 m*M* Tris buffer, pH 8.0, on Q Sepharose FF.

teristic charge z_{BSA} is 5.61. This value is slightly higher than the value of 3.5 reported by Bosma and Wesselingh [15] and 3.1 reported by Whitley et al. [12]. The correlated negative charge of myoglobin was 0.92. This value is in the range of 0.6–1.3 as reported for adsorption of myoglobin unto various ion-exchangers at pH 4–5 by Whitley et al. [12]. These observations support the conclusion drawn by Bosma and Wesselingh [15], that the protein has a constant binding charge, which is predominantly determined by steric factors instead of pH effects.

From the retention times under non-retaining conditions, i.e. in 1 *M* NaCl, the fraction of the pores accessible to the protein molecules was calculated, assuming a bed porosity, ϵ_b, of 0.4. For the larger BSA molecule (M_r 68 000), only 49% of the particle volume is accessible. The fraction of the total bed accessible to BSA is 69%, which is close to the 70% reported by Bosma and Wesselingh [15]. The smaller myoglobin molecule (M_r 18 000) can penetrate into 64% of the particle volume (Table 2). The small NaCl molecule was assumed to be able to penetrate in the entire particle; possible exclusion effects were included in the ion-exchange equilibrium coefficient.

Breakthrough experiments were used to verify the pulse equilibrium data and to estimate mass transfer parameters. A good agreement between the experimental and simulated breakthrough curves of BSA was found when the equilibrium data from pulse experiments and 20 discretization steps were used (see Fig. 4A). The agreement of the experimental and simulated breakthrough curves of myoglobin was bad (see Fig. 4B). A possible explanation is that the breakthrough curves were determined in much higher salt concentrations (200–300 m*M*) than used during pulse experiments (4–100 m*M*). We decided to use the equilibrium coefficients fitted from the breakthrough curves, because the SMB experiments were also done at high salt concentrations. The equilibrium data used in further processing are given in Table 2.

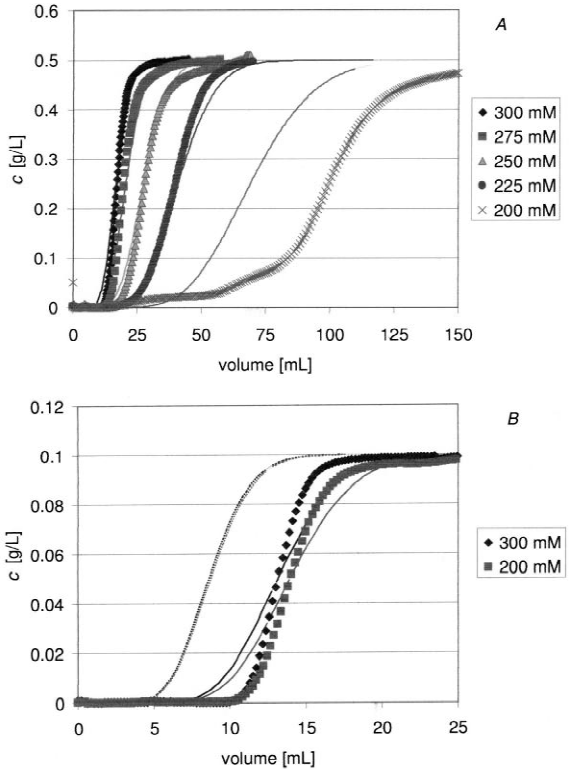

Fig. 4. Measured and simulated breakthrough curves of BSA (A) and myoglobin (B). In the latter figure, dotted lines indicate simulations using equilibrium data obtained from pulse experiments, drawn lines indicate simulations using the equilibrium data given in Table 2.

4.2. Upward gradient

4.2.1. Region of complete separation

The boundaries to the region of complete separation of an upward gradient using $c_D = 0.27$ *M* and $c_F = 0.15$ *M* were determined using the experimental distribution coefficients given in Table 2. The resulting lines are shown in Fig. 5. Their origin and their implications are

- positive feed: only above this line, feed can be added
- $m_2$min NaCl: on this line, m_2 equals the slope of the salt isotherm at concentration $c_{II=}c_D$. The line is straight, since c_D is constant. Only at m_2 exceeding this value, NaCl moves upward in section II
- $m_2$max BSA: on this line, m_2 equals the distribution coefficient of BSA at concentration c_D. Only at m_2 smaller than this value, BSA moves downward in section II
- $m_2$min myo: on this line, m_2 equals the distribution coefficient of myoglobin at concentra-

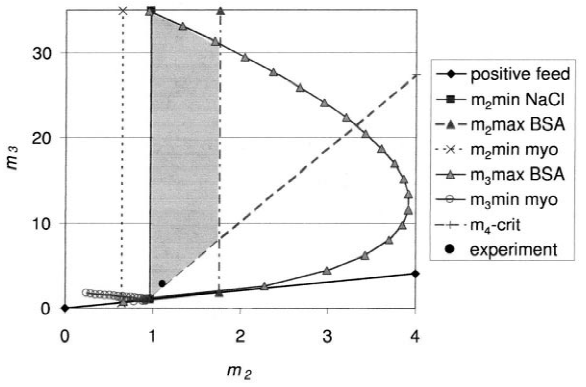

Fig. 5. Region of complete separation in case of an upward gradient, using $c_F = 0.15$ *M* and $c_D = 0.27$ *M* NaCl. Complete separation is possible in the shaded area. The symbol indicates the experiment (cf. Table 3).

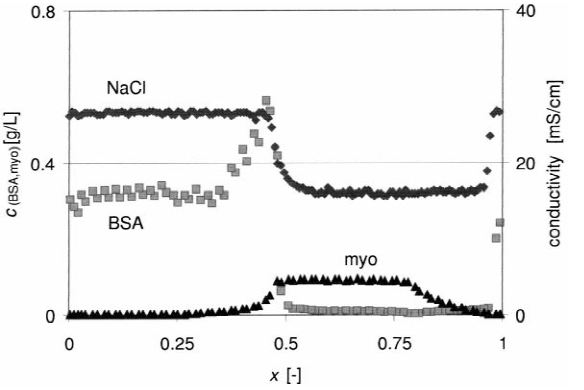

Fig. 6. Profile at half switch time during a downward gradient experiment (conditions in Table 3).

tion c_D. Only at m_2 exceeding this value, myoglobin moves upward in section II

- $m_3$max BSA:on this line, m_3 equals the distribution coefficient of BSA at concentration c_{III}, which is calculated from the feed mass balance (1). The line is curved, since c_{III} varies over the line. Only at m_3 smaller than this value, i.e. inside the curve, BSA moves downward in section III
- $m_3$min myo:on this line, m_3 equals the distribution coefficient of myoglobin at concentration c_{III}, calculated from the feed mass balance (1). Only at m_3 larger than this value, i.e. outside the curve, myoglobin moves upward in section III
- m_4 crit: on this line, defined by (3), c_{III} equals the concentration at intersection of the myoglobin and NaCl isotherm ($c_{crit,IV}$) which equals 0.16 *M* at the chosen desorbent concentration. Only at combinations of m_2 and m_3 to the left of this line, regeneration of the desorbent in section IV is established since the c_{III} is then below this critical concentration.

From these observations it is concluded that complete separation is only possible in the shaded area depicted in Fig. 5. Due to the lower concentration of salt in section III compared to section II, a high feed flow-rate can be applied and a high throughput can be achieved. The shape of the region closely resembles the previously reported one [10]. However, instead of the less retained protein, salt now governs the minimal m_2, as a result of interaction of the salt with the sorbent.

Note that this region of complete separation does not provide complete guidelines for correct choice of m_1 or m_4. The flow-rate ratio m_1 should exceed the maximum equilibrium coefficient in section I (cf. Table 1) to enable regeneration of the sorbent. The flow-rate ratio m_4 should be between the distribution coefficient of salt and myoglobin at salt concentration c_{III} to enable regeneration of the desorbent.

4.3. Verification by experiment

Fig. 6 and Table 3 show that the upward salt gradient was well positioned at the experimental point indicated in Fig. 5. Note that Fig. 6 does not show a profile over the SMB. Instead, the ex-

Table 3
Conditions and observed directions of movement of components during upward gradient experiment, with $c_D = 0.27$ *M*, $c_F = 0.15$ *M* and $\tau = 250.9$ s

Section	*m*	Movement of components		
		NaCl	BSA	myo
I	2.11	Up[a]	Down	Up[a]
II	1.12	Up[a]	Down[a]	Up[a]
III	3.07	Up[a]	Down[a]	Up[a]
IV	1.09	Up[a]	Down[a]	Up[a]

[a] Directions of movement indicate agreement between experiment and prediction.

perimental points at half switch time are plotted at equal distance, thus assuming a constant species velocity in all section. Hence, the figure can only be interpreted as ''the front enters a section, not knowing how far''. This figure allows an easy determination of the achievement of steady state from the detector signal.

In all sections, downward movement of BSA was observed. In sections II–IV, this agreed well to the theoretical prediction, because the experimental point was well below the $m_2$max BSA and the $m_3$max BSA lines and m_4 was chosen well below the calculated distribution coefficient at the predicted salt concentration. The experimental behavior of BSA in section I could not be understood on the basis of equilibrium theory. On basis of the flow-rates and distribution coefficients, the anticipated movement of BSA in section I was upward, whereas downward movement was observed. No explanation for this behavior could be verified. However, we think pH effects may have contributed, since the ion-exchange of proteins is a strong function of pH and the pH on the ion-exchanger varies in a salt gradient [16]. In the experimental SMB system, the pH could not be monitored.

The experimental upward movement of myoglobin in sections I–IV agreed very well with the theoretical predictions (cf. Table 3). The experimental flow-rate ratios in sections II and III were chosen well above $m_2$min myo and $m_3$min myo, respectively. The salt concentration $c_{III}=0.16$ M was slightly below $c_{crit,IV}$, which agreed to the position relative to the $m_{4,crit}$ line in Fig. 5. In principle regeneration of the desorbent would have been possible. However, the value of m_4 (1.09) was chosen above the distribution coefficient of myoglobin at that concentration (0.94), resulting in upward movement. Also, m_1 exceeded the distribution coefficient at the calculated concentration.

The results indicate that a situation of complete separation can well be established after selection of the flow-rates using the developed method.

4.4. Downward gradient

4.4.1. Region of complete separation

The boundaries to a region of complete separation of a downward gradient were calculated at $c_D=0.22$ M, $c_F=0.31$ M and $m_1=0.88$, using the equations given in Table 2. The choice of salt concentration was only determined by the possibility to achieve complete separation of the two components in sections II and III, whereas the choice of m_1 was only determined by the salt movement in section I. The resulting boundaries are shown in Fig. 7. In each of these, the salt concentrations c_{II} and c_{III} were computed from the feed and desorbent mass balances (1) and (2). The meaning and the implications of the boundaries are (similar to those in Fig. 5)

- positive feed: only above this line, feed can be added
- $m_2$max BSA: on this line, m_2 equals the distribution coefficient of BSA at concentration c_{II}. The line is curved, since c_{II} is a function of m_2 and m_3 chosen. Only below this line, BSA moves downward in section II
- $m_2$min myo: on this line, m_2 equals the distribution coefficient of myoglobin at concentration c_{II}. Only above this line, myoglobin moves upward in section II
- $m_3$max NaCl: on this line, m_3 equals the chord of the salt isotherm between concentrations c_{II} and c_D. Only below this line, salt moves downward in sections III and IV
- $m_3$max BSA: on this line, m_3 equals the distribution coefficient of BSA at concentration c_{III}. The line is curved, since c_{III} varies over the line.

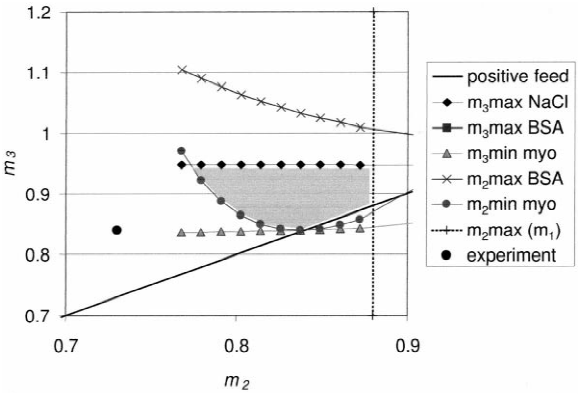

Fig. 7. Region of complete separation (lines and small markers) and experiment (large ○) in case of a downward gradient, using $c_F=0.22$ M, $c_D=0.31$ M NaCl and $m_1=0.88$. Complete separation in sections II and III is obtained in the shaded area, however regeneration of the sorbent in section I is not established.

Only below this line, BSA moves downward in section III. The curve is not shown in Fig. 6, since it is found at high m_3

- $m_3$min myo: on this line, m_3 equals the distribution coefficient of myoglobin at concentration c_{III}. Only above the curve, myoglobin moves upward in section III
- $m_2$max(m_1): only to the left of this line, an extract stream can be withdrawn ($m_1 > m_2$).

This latter line could be regarded as an artifact, that results of an incorrect choice of m_1. At correct choice of m_1, the minimum allowed m_1 equals the maximum allowed $m_2 = K_{BSA}(c_{II})$, so $m_1 > m_2$ per definition. Whenever m_1 is chosen too low, its value restricts m_2.

Complete separation in sections II and III is only possible in the shaded area in Fig. 7. The chosen salt concentrations do not support regeneration of the sorbent in section I, because the critical salt concentration $c_{crit,I} = 0.32$ *M* cannot be reached using $c_F = 0.31$ *M*. The critical salt concentration was obtained by equating the slope of the salt isotherm between $c_D = 0.22$ *M* and $c_{crit,I}$ to the BSA distribution coefficient at $c_{crit,I}$. Correct functioning of section I will be elaborated in a later paragraph.

4.5. Verification by experiment

Fig. 8 shows that the downward salt gradient was very well positioned using the experimental conditions of Table 4, represented by the experimental point in Fig. 7. This is expected, because the point is well below the $m_3$max NaCl line indicated in Fig. 7.

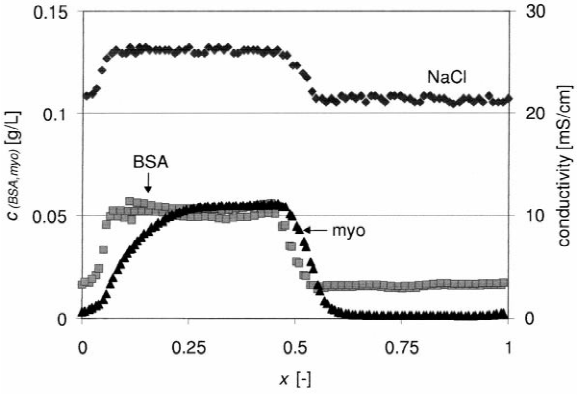

Fig. 8. Profile at half switch time during a downward gradient experiment (conditions in Table 4).

Table 4
Conditions and observed directions of movement of components during downward gradient experiment, with $c_D = 0.22$ *M*, $c_F = 0.31$ *M* and $\tau = 150.9$ s

Section	*m*	Movement of components		
		NaCl	BSA	myo
I	0.88	Down[a]	Down[a]	Up[a]
II	0.73	Down[a]	Down[a]	Down[a]
III	0.84	Down[a]	Down[a]	Down
IV	−0.05	Down[a]	Down[a]	Down[a]

[a] Directions of movement indicate agreement between experiment and prediction.

Complete separation of BSA and myoglobin did not occur; myoglobin contaminated the extract. This can be explained by the position of the experimental point relative to the $m_2$min myo line; m_2 was chosen at a too low value, and consequently myoglobin moved downward in section II. In section III, the movement of myoglobin was predominantly downward. The point is above the $m_3$min line, so theory predicts upward movement (Table 4). However, only by a slight experimental error in flow-rates or salt concentrations, the direction of movement is likely to be reverted, because the experimental point is very close to the $m_3$min myo line.

BSA moved downward in both sections II and III. This is understood from the position of the experimental point, which is well below the $m_2$max BSA and $m_3$max BSA lines.

In section IV, all components moved downward, which is explained by the very low value of m_4 chosen. In section I, BSA moved downward, which is also predicted at the experimental salt concentrations and flow-rate ratios. The downward movement of BSA in section I had the result that the sorbent was not properly regenerated. Hence, BSA was transported along with the sorbent to section IV. This explains the high concentrations of BSA seen in sections III and IV in Fig. 8.

4.6. Regeneration of sorbent

A second region of complete separation was constructed for a downward gradient operated under conditions that support regeneration of the sorbent in

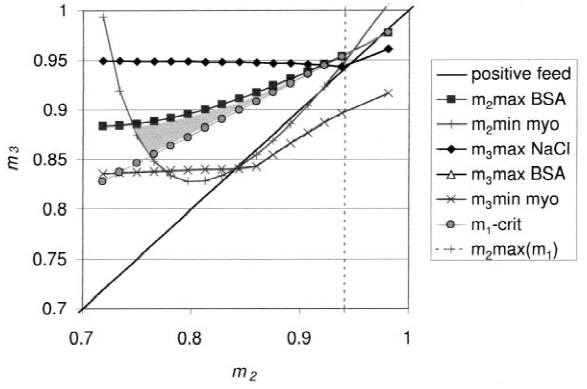

Fig. 9. Region of complete separation in case of a downward gradient, using $c_F = 0.45$ *M*, $c_D = 0.22$ *M*, and $m_1 = 0.94$. Complete separation is only possible in the shaded area.

section I. Fig. 9 shows the result at $c_F = 0.45$ *M*, $c_D = 0.22$ *M*, and $m_1 = 0.94$. At this combination of salt concentrations and m_1, the salt concentration $c_{crit,I}$ necessary for sorbent regeneration can in principle be reached. The actual realization of that concentration depends on m_2 and m_3; hence an additional constraint is found, which implies:

- m_1 crit: on this line, given by (4), c_{II} equals the concentration at intersection of the BSA and NaCl isotherm, $c_{crit,I} = 0.32$ *M* at the corresponding c_D. Only at combinations of m_2 and m_3 to the left of this line, c_{II} exceeds this critical concentration, and downward movement of NaCl as well as upward movement of the proteins is established.

This additional criterion strongly reduces the region of complete separation.

In Fig. 9, the $m_2\max(m_1)$ line no longer imposes a constraint to the region, as it did in Fig. 7. This is the result of correct selection of m_1 (cf. explanation in Fig. 7).

Fig. 9 does not provide guidelines for selection of m_4. The flow-rate ratio m_4 can have any value below the minimal distribution coefficient at c_{III}, in order to move all components downward and regenerate the desorbent.

4.7. Center gradient

Correct positioning of the salt gradient is essential to be able to separate the proteins. However, even experiments with wrongly positioned salt gradients should support the theory for movement of the proteins. In the three experiments listed in Table 5, the salt gradient was not correctly positioned. Fig. 10 shows the center gradient obtained during experiment 3 as an example.

Complete separation can no longer be predicted on the basis of Table 2, as the salt concentrations are incorrectly predicted by the mass balance Eqs. (1) and (2), that assume a correct (downward) gradient.

Table 5
Conditions and observed directions of movement of components during center gradient experiments, with $c_D = 0.22$ *M*, $c_F = 0.31$ *M* and $\tau = 150.9$ s

Exp.	Section	m_s	c (*M*)	Movement of components		
				NaCl	BSA	myo
1	I	0.95	0.22–0.29	Up	Down[a]	Up[a]
	II	0.71	0.29	Down[a]	Down[a]	Down[a]
	III	0.95	0.29–0.22	Down[a]	Down[a]	Up[a]
	IV	−0.34	0.22	Down[a]	Down[a]	Down[a]
2	I	0.93	0.22–0.2	Down[a]	Down[a]	Up[a]
	II	0.75	0.29	Down[a]	Down[a]	Down[a]
	III	0.98	0.29–0.22	Up	Up	Up[a]
	IV	−0.28	0.22	Down[a]	Down[a]	Down[a]
3	I	0.98	0.22	Up[a]	Up	Up[a]
	II	0.89	0.30	Down[a]	Down[a]	Up[a]
	III	1.01	0.30–0.22	Up[a]	Up	Up[a]
	IV	0.11	0.22	Down[a]	Down[a]	Down[a]

[a] Directions of movement indicate agreement between the experiment and the direction of movement predicted at the salt concentrations calculated by a TMB equilibrium stage model.

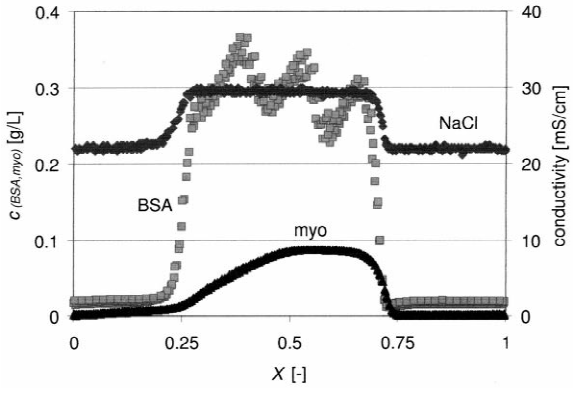

Fig. 10. Profile at half switch time during center gradient experiment 3 (conditions in Table 5).

In order to verify the movement of components, we used a steady state TMB model to calculate the salt concentrations.

Using the calculated salt concentrations, the upward movement of myoglobin in sections I–III, as well as the downward movement of BSA in section II and the downward movement of both components in section IV in experiment 3 were well predicted (cf. Table 5). The upward movement of BSA in section III could not be understood. Neither were the oscillations in the BSA signal.

Also in the other center gradient experiments, the observed directions of movement of the proteins agreed well to those predicted at the calculated concentrations of salt (cf. Table 5). This supports the developed method for flow selection.

5. Conclusions

This paper describes the fractionation of a dilute binary mixture of proteins using salt gradient SMB. A method for flow-rate selection is developed based on ''triangle theory'' [7]. The procedure ensures complete separation of the proteins as well as regeneration of the sorbent in section I and regeneration of the desorbent in section IV. Therefore, it includes the correct positioning of the salt gradient as described in [14]. The separation of the proteins is ensured by adjusting the flow-rate ratio to the distribution coefficient of the protein at the concentration of salt that is calculated at those flow settings. The regeneration of the sorbent and desorbent is ensured by realization of a critical salt concentration in sections I and IV. Due to the intersection of the salt and protein distribution coefficients as a function of the salt concentration, the salt concentration in section I has to exceed a critical salt concentration $c_{\mathrm{crit,I}}$ in case of a downward gradient, whereas the salt concentration in section IV needs to be lower than the critical salt concentration $c_{\mathrm{crit,IV}}$ in case of an upward gradient. These critical concentrations impose additional demands on both the desorbent-and feed concentration, as well as the flow-rate ratios in all sections.

The equilibrium and mass parameters of BSA and myoglobin on Q-Sepharose FF at pH 8.0 were obtained from pulse and breakthrough experiments. The operating regions calculated using these parameters could be verified by experiments. In both upward, downward and center gradients, the experimental movement of components agreed fairly well to the movement predicted on the basis of the location relative to the region of complete separation.

6. Nomenclature

a	specific interfacial area (1/m)
c	concentration in the liquid phase (M)
D	diffusion coefficient (m^2/s)
d_p	particle diameter (m)
K	distribution coefficient (−)
k_o	mass transfer coefficient (m/s)
m	flow-rate ratio (−)
q	concentration in the sorbed phase (M)
Q	ion-exchange capacity of the resin (mol/l)
t	time (s)
V	volume of one column (l)
V_d	dead volume per column (l)
x	distance (m)
z	ionic charge (C/mol)

Greek symbols

β	phase ratio, $(1-\epsilon_b)/\epsilon_b$ (−)
ϵ_b	bed porosity (−)
ϵ_p	accessible pore fraction (−)
Φ	flow-rate (l/s)
τ	switch time (s)

Super- and subscripts
D desorbent
eq at equilibrium
F feed
j section number (I, II, III, IV)
p protein
s salt

Acknowledgements

The Dutch ministry of Economic Affairs (through Senter) has financially supported this research in the framework of IOP-milieu preventie. The authors thank Thomas Jensen for many stimulating discussions and Bart van Beek and Dirk Geerts for the experimental isotherm determination.

References

[1] M. Juza, M. Mazzotti, M. Morbidelli, Tibtech. 18 (2000) 108.
[2] M. Schulte, J. Strube, J. Chromatogr. A 906 (2001) 399.
[3] H.J. Van Walsem, M.C. Thompson, J. Biotechnol. 59 (1997) 127.
[4] T.B. Jensen, T.G.P. Reijns, H.A.H. Billiet, L.A.M. van der Wielen, J. Chromatogr. A 873 (2000) 149.
[5] B. Ballanec, G. Hotier, in: G. Ganetsos, P.E. Barker (Eds.), Preparative and Production Scale Chromatography, Marcel Dekker, New York, 1993.
[6] Z. Ma, N.-H.L. Wang, AIChE. J. 43 (1997) 2488.
[7] G. Storti, M. Mazzotti, M. Morbidelli, S. Carrà, AIChE. J. 39 (1993) 471.
[8] D.M. Ruthven, C.B. Ching, Chem. Eng. Sci. 44 (1989) 1011.
[9] M. Mazzotti, G. Storti, M. Morbidelli, J. Chromatogr. A 786 (1997) 309.
[10] J. Houwing, H.A.H. Billiet, J.A. Wesselingh, L.A.M. van der Wielen, J. Chem. Technol. Biotechnol. 74 (1999) 213.
[11] W. Kopaciewitz, M.A. Rounds, J. Fausnaugh, F.E. Regnier, J. Chromatogr. 226 (1989) 3.
[12] R.D. Whitley, R. Wachter, F. Liu, N.-H.L. Wang, J. Chromatogr. 465 (1989) 13.
[13] C.A. Brooks, S.M. Cramer, AIChE. J. 38 (1992) 1969.
[14] J. Houwing, T.B. Jensen, S.H. van Hateren, H.A.H. Billiet, L.A.M. van der Wielen, AIChE. J. (2001) submitted for publication.
[15] J.C. Bosma, J.A. Wesselingh, AIChE. J. 44 (1998) 2399.
[16] M.L. Jansen, A.J.J. Straathof, L.A.M. van der Wielen, K.Ch.A.M. Luyben, W.J.J. van den Tweel, AIChE. J. 42 (1996) 1911.
[17] C. Migliorini, M. Mazzotti, M. Morbidelli, AIChE. J. 45 (1999) 1411.
[18] F.G. Helfferich, G. Klein, Multicomponent Chromatography: Theory of Interference, Marcel Dekker, New York, 1970.
[19] Pharmacia Biotech, Ion-Exchange Chromatography: Principles and Methods, Västra Aros tryckeri AB9511, Sweden, 1996.
[20] J. Houwing, H.A.H. Billiet, L.A.M. van der Wielen, AIChE. J. (2001) submitted for publication.